Electrical Control of Silicon Photonic Crystal Cavity by Graphene

Arka Majumdar,[†,‡,∥] Jonghwan Kim,[†,∥] Jelena Vuckovic,[‡] and Feng Wang*[,†,§]

[†]Department of Physics, University of California at Berkeley, Berkeley, California 94720, United States

[‡]E. L. Ginzton Laboratory, Stanford University, Stanford, California 94305, United States

[§]Materials Science Division, Lawrence Berkeley National Laboratory, Berkeley, California 94720, United States

S Supporting Information

ABSTRACT: The efficient conversion of an electrical signal to an optical signal in nanophotonics enables solid state integration of electronics and photonics. The combination of graphene with photonic crystals is promising for electro-optic modulation. In this paper, we demonstrate that by electrostatic gating a single layer of graphene on top of a photonic crystal cavity, the cavity resonance can be changed significantly. A ~2 nm change in the cavity resonance line width and almost 400% (6 dB) change in resonance reflectivity is observed. In addition, our analysis shows that a graphene–photonic crystal device can potentially be useful for a high speed and low power absorptive and refractive modulator, while maintaining a small physical footprint.

KEYWORDS: Graphene, photonic crystal cavity, electro-optic modulation
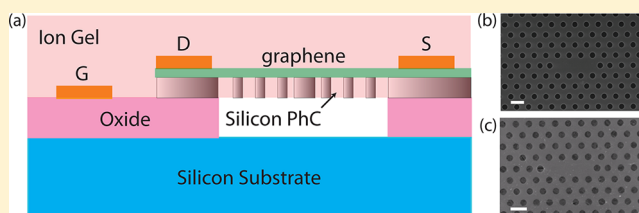
Integrating photonics and electronics on the same platform holds great promise for the future of high-performance computing.[1] However one of the major challenges to bring optics and electronics together is the efficient conversion between the optical and electronic signal, that is, designing fast, low power electro-optic modulators as well as fast, sensitive photodetectors. Developing compact and power-efficient electro-optic modulator requires progress in two directions: new optical material with strong and field-tunable optical transitions, and new nanophotonic design with resonantly enhanced light–matter interactions in a small mode volume.

Optical properties of graphene, a two-dimensional material with linear dispersion and zero electron density of states at the Dirac point, can be easily controlled by applying an electric field.[2,3] Hence graphene is a very attractive candidate for performing electro-optic modulation. Recent studies have demonstrated efficient electro-optic modulation in silicon waveguide integrated with graphene (switching contrast of 0.1 dB μm^{-1}).[4] However, the size required for the waveguide to achieve a good switching contrast is large, as light needs to travel a long distance overlapping with graphene. One can greatly enhance the light–graphene interaction and reduce the size of the optical modulator by coupling graphene to a photonic crystal cavity with high quality (Q) factor. Indeed the excellent electrical transport properties and nanofabrication capability can enable such integrated device for ultrahigh speed and low power operation in a small footprint. Very recently it has been shown that graphene can modify the photonic crystal cavity resonance and give rise to interesting nonlinear optical phenomena. However, no electrical control of such graphene–cavity system has been demonstrated.[5,6] Several other proposals involve using graphene in distributed Bragg reflector cavity[7] or

metallic Fabry–Perot cavity[8] for enhancing light–matter interaction, but the cavities used were of high mode volume and relatively lower quality factor (~20−95). During preparation of the manuscript we became aware of a similar experiment where the resonance of a slot waveguide photonic crystal cavity is changed by ion-gel gating of graphene.[9] In this paper, we report electrical control of a silicon photonic crystal cavity (quality factor of ~1000−1500 and mode volume ~$(\lambda/n)^3$, n being the refractive index of the cavity material) through electrostatic gating of a monolayer graphene on top of it. We show that, although graphene is only one atom thick, its effect on the photonic crystal cavity is remarkably strong: both the cavity resonance line width as well as the cavity reflection can be modulated significantly.

Effect of Graphene. The experiments are performed with linear three hole defect (L3) silicon photonic crystal cavities fabricated in silicon-on-insulator (SOI) platform. The device thickness d is 250 nm, with photonic crystal lattice periodicity a = 450 nm and radius r = 90 nm. The two holes at the end of the cavities are shifted by $0.15a$.[10] The photonic crystals are fabricated by electron-beam lithography, followed by plasma etching and finally removing the silicon oxide underneath to make a free-standing silicon photonic crystal membrane. On top of the cavities we transferred a large-area graphene grown by chemical vapor deposition using the standard growth and transfer processes.[11,12] For electrostatic gating of graphene we used a top electrolyte gating with ion-gel.[13] The device schematic is shown in Figure 1a. Figure 1b and c are scanning

electron micrograph images of a fabricated photonic crystal cavity before and after the graphene transfer, respectively.
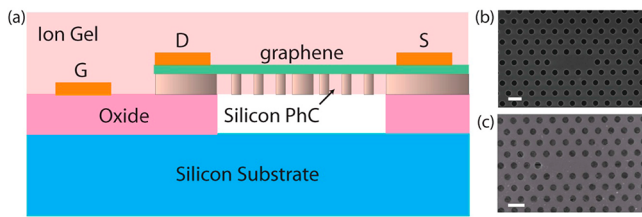
Figure 1. (a) Schematic of the photonic crystal cavity–graphene device. The cavity is fabricated on a silicon-on-insulator platform, and the electrical gating is performed by means of contacts (drain, source, and gate) covered by an ion-gel. (b,c) Scanning electron micrograph (SEM) of the fabricated cavities (b) without and (c) with graphene. The scale bars correspond to a 500 nm distance.

We characterize the photonic crystal cavities in cross-polarized reflectivity measurement setup with a broadband light-source (a supercontinuum laser), where the cavity is kept at a 45° angle, the incident probe laser is vertically polarized, and we collect horizontally polarized light.[14] Collected light is analyzed by a spectrometer equipped with an InGaAs array detector. A quality (Q) factor of ∼1000−1500 is observed for the fabricated cavities without graphene. We note that, although a much higher quality factor can be obtained in a silicon photonic crystal cavity, we want to keep the quality factor moderate to achieve a relatively large spectral bandwidth. With graphene on top, the Q-factor drastically reduces to ∼300−500, as shown in Figure 2a. The significant broadening of the cavity
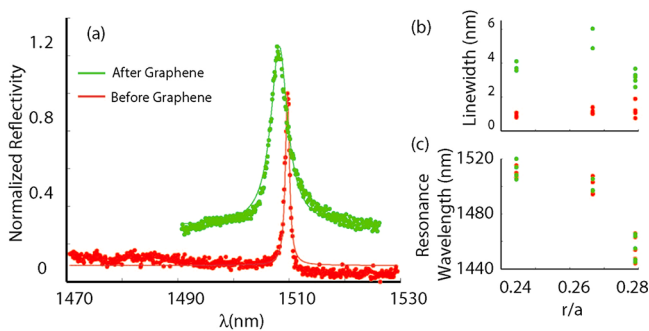
Figure 2. Cavity reflectivity spectrum measured in the cross-polarized reflectivity setup: (a) Normalized reflectivity spectrum from a cavity before (red plot) and after (green plot) graphene transfer. A significant broadening of the cavity is observed due to graphene absorption. The two plots are vertically offset for clarity. (b) The linewidths of cavities as a function of r/a of the photonic crystal measured for several different cavities in three sets of cavities with different r/a. The uncertainty in the line width from the fitting is less than 0.2 nm. (c) The cavity resonance wavelength as a function of r/a of the photonic crystal. The green and red dots, respectively, correspond to the situations after and before graphene transfer (both in b and c).

line width arises from graphene absorption. We measured the reflectivity spectrum from several cavities with a slightly different r/a ratio. For all the cavities we consistently observe line-width broadening (Figure 2b). The quantitative values of the broadening varies slightly in the range of 2−4 nm, consistent with our theoretical estimation (Supporting Information) and the recent experimental observations.[6]

Change in the cavity resonance frequency is quite small, and no consistent behavior is observed (Figure 2c).

Effect of Electric Field. Then we study the effect of the electric field on the graphene–cavity device. We gate the graphene layer by means of the ion-gel (refractive index ∼1.43)[15] that we spin-coat on the device. Figure 3 shows the effect of the electric field on the graphene–cavity device. We simultaneously measure the cavity reflection spectrum and graphene resistance while varying the gate voltage at a step of 10 mV/s. Figure 3a shows the cavity reflectivity spectra for different voltages. A narrowing in the cavity line width as well as an increase in the cavity reflectivity is clearly observed with increasing gating of the graphene. We fit all of the spectra with a Lorentzian line-shape to extract the cavity resonance frequencies and cavity linewidths. Figure 3b shows the peak value of the cavity reflectivity as a function of the applied voltage. Figure 3c,d show the cavity linewidths and the resonance frequencies as a function of the applied voltage. Figure 3e shows the resistance between the drain and the source as a function of the gate voltage. From the transport data (Figure 3e) we clearly observe that graphene charge neutral point (the point where the resistance is maximum) is at around 0.5 V. The small deviation from the 0 V is due to slight p-doping of graphene during the graphene transfer process. We observe narrowing of the cavity line width and an increase in the cavity reflection consistent with the fact that increased gating of the graphene reduces its absorption. The change in the cavity resonance is relatively small. We confirmed that, in this voltage range, the ion gel does not affect the cavity resonance (data not shown here).

Theory. To conclusively prove that the change in cavity resonances are solely due to graphene, we theoretically fit our experimental observations. Gate-dependent complex dielectric constant of graphene has been extensively studied previously.[16−18] The complex dielectric function $\varepsilon_g(\omega)$ can be obtained from the optical conductivity $\sigma(\omega) = \sigma_1(\omega) + i\sigma_2(\omega)$ of graphene by using: $\varepsilon_g(\omega) = 1 + i\sigma(\omega)/(\omega\varepsilon_o d_g)$, where d_g is the thickness of the graphene layer (we used $d_g \sim 1$ nm in our fit). Under random phase approximation and using the Kramer−Kronig relation, we can write the real and imaginary part of the optical conductivity as:

$$\sigma_1(\omega) = f(\omega) + \frac{q^2\Gamma}{2\pi\hbar^2}\frac{1/\tau}{\omega^2 + (1/\tau)^2}\log\left(2\cosh\frac{2E_F}{\Gamma}\right)$$

$$\sigma_2(\omega) = -\frac{q^2}{8\hbar}\frac{2\omega}{\pi}\int_\infty^0 \frac{f(\omega') - f(\omega)}{\omega'^2 - \omega^2}d\omega + \frac{q^2\Gamma}{2\pi\hbar^2}$$
$$\frac{\omega}{\omega^2 + (1/\tau)^2}\log\left(2\cosh\frac{2E_F}{\Gamma}\right)$$

with

$$f(\omega) = \frac{q^2}{8\hbar}\left[\tanh\left(\frac{\hbar\omega + 2|E_F|}{\Gamma}\right) + \tanh\left(\frac{\hbar\omega - 2|E_F|}{\Gamma}\right)\right]$$

and q is the electronic charge and Γ is the interband transition broadening (estimated to be 150 meV from the fitting). The free carrier scattering rate $1/\tau$ can be neglected because it has little effect on the dielectric constants at the vicinity of the cavity resonance energy ($E_r = \hbar\omega_r$). From these equations we find that $\sigma_1(\omega)$ decreases when $2|E_F|$ is larger than E_r and blocks the relevant interband transitions. $\sigma_2(\omega)$ has significant contribution both from intraband and interband transition.
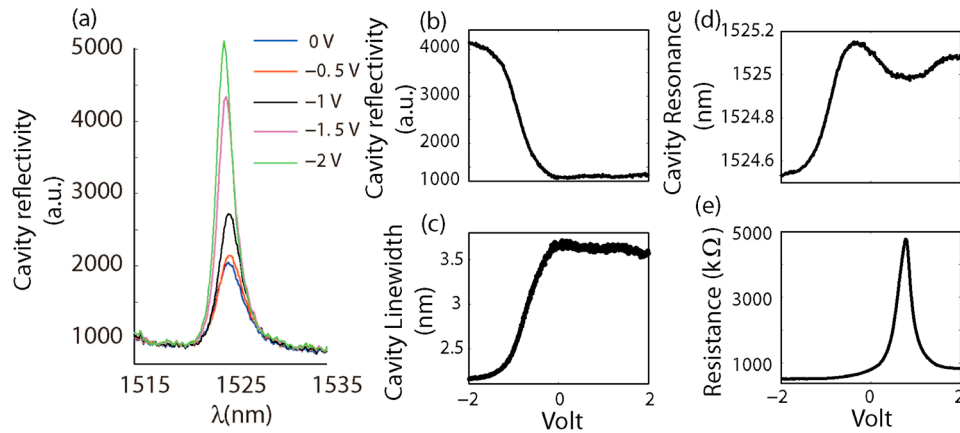
Figure 3. Effect of electric field on graphene−cavity device: (a) Cavity reflectivity spectra for several voltages. An increase in cavity reflectivity and narrowing of cavity line width is observed with increased gating of the graphene. (b) The peak reflectivity of the cavity; (c) the cavity line width; (d) the cavity resonance; and (e) the resistance measured between the source and the drain as a function of the gate voltage.

Contribution from the intraband transition $[(q^2\Gamma/2\pi\hbar^2)(\omega/(\omega^2 + (1/\tau)^2))\log(2\,\cosh(2E_F/\Gamma))]$ increases monotonically with increasing $|E_F|$, that is, with increasing carrier density. On the other hand, interband transition contribution has a minimum at $2|E_F| = E_r$. We note that in our experiment we are applying a voltage V to the graphene layer, and the Fermi level of graphene and applied voltage can be related by the formula[19,20]

$$E_F = \hbar v_f \sqrt{\pi\left(n_o + \frac{C|V|}{q}\right)}$$

where C is the effective capacitance per unit area, v_f is the Fermi velocity for graphene, and n_o is the intrinsic carrier concentration. The effective capacitance of ion gel gating is $C \sim 20$ mF/m^2;[13,16,21,22] Fermi velocity $v_f = 10^6$ m/s, and any intrinsic carrier concentrations are neglected. Figure 4a,b shows
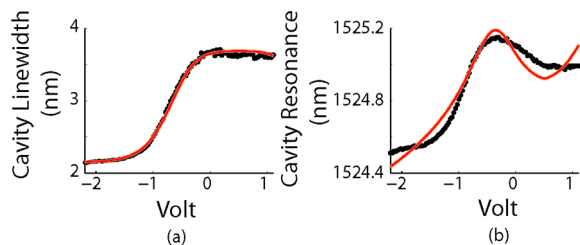
Figure 4. Theoretical fit to the experimental data: (a) cavity line width and (b) cavity resonance as a function of the applied voltage. The decreasing cavity line width can be explained by the imaginary part of the graphene dielectric constant, whereas the change in the cavity resonance can be explained by the real part of the graphene dielectric constant.

the cavity line width and the cavity resonance wavelength as a function of the applied voltage. We found that the shift (both blue and red) and the line-width increase of the cavity resonance scale linearly with the gate-dependent dielectric constant of graphene. The theoretical fits in Figure 4a,b (red solid line) are obtained by the following relations: for the cavity line width $\Gamma_R = \Gamma_R^0 + \alpha\text{Im}[\varepsilon_g(\omega)]$ and for the cavity resonance wavelength $\lambda_R = \lambda_R^0 + \beta\text{Re}[\varepsilon_g(\omega)]$. Our simple model reproduces nicely the significant gate-induced decrease of cavity line-width, as well as the shift (both blue and red) in the

cavity resonance frequencies. We note that the line width narrowing observed by gating graphene is ~1.5 nm, which matches the theoretical estimate of the change in the line width just due to the graphene absorption (Supporting Information).

Performance of the Modulator. In this paper, we have used ion-gel to electrostatically dope graphene to demonstrate the capability to modulate the cavity resonance by gating graphene. However, ion-gel gating cannot be used in high speed electro-optic modulator due to the slow response of ions under the electric field. Instead, one should employ semiconductor field-effect transistor structure to gate graphene and achieve ultrafast electro-optic modulation. Here, we theoretically analyze the performance (speed and energy consumption) of such a graphene-photonic crystal cavity modulator with silicon gating. Assuming we need a specific carrier density of n_c (charge/area) to cause significant change in the graphene absorption, we can write $n_c = CV/q$, where q is the electronic charge, V is the applied voltage, and $C = \varepsilon/d$ is the capacitance per unit area, and d is the alumina thickness. The total capacitance will be $C_T = CA$, with A being the gated graphene area. Hence the total energy E_T consumption for the modulator will be $1/2C_TV^2$. This means

$$E_T = \frac{1}{2}CAV^2 = \frac{Aq^2n_c^2d}{2\epsilon}$$

In a graphene−PhC modulator we can achieve: $A = 1$ μm^2 (assuming that the lithographically defined graphene covers only the cavity region), alumina thickness $d = 5$ nm, dielectric constant of alumina is 10, and the carrier density in graphene required to do such modulation is 10^{17}/m^2, then the capacitance of the device becomes $C_T = 17$ fF. Such a low capacitance is the key for low energy and high speed operations. For high-frequency operations, the parasitic capacitance of the metal wire on the alumina on silicon will limit the performance. To circumvent that, one needs to dope the silicon selectively and reduce the overlap between graphene and doped silicon only to the cavity region.

With a device capacitance of 17 fF, the energy of the modulator is around 8 fJ. The speed of the device will be limited by the RC constant of the device. The resistance of the device will come mostly from the graphene resistance, assuming the silicon is highly doped, and is of very low resistance. Again, one needs to bring the electrodes closer to the cavity to reduce

the resistance. Such nanofabrication is already demonstrated in GaAs photonic crystal cavity[23] and can be easily extended to the SOI platform. In our device, the graphene resistance is around 500 Ω (including the contact resistance), leading to a device speed of ∼20 GHz. However, the dc conductivity of graphene in strongly doped region, as used in the modulator condition,[4] can be quite high. Sukang et al. has shown a sheet resistivity of 30 Ω/sq.[24] Assuming the length and width of the graphene electrode are ∼1 μm, we find that the resistance of the device can be as low as 30 Ω, and the speed of the modulator can be over 100 GHz.

Conclusion. In summary, we observe drastic changes in the parameters of a photonic crystal cavity by electrostatic gating of the graphene on top of it. A line width narrowing of 1.5 nm is observed, along with around 1 nm shift in cavity resonance and a 6 dB change in cavity reflectivity. Using a cavity we significantly reduce the physical footprint for the device compared to a waveguide-based modulator. Our analysis shows that such a graphene-cavity based modulator can be used for very low power (fJ) electro-optic modulation maintaining a speed of hundreds of GHz. We believe that such electrically controlled graphene-cavity device will enable technologies that benefit from local fast electrical tuning of cavities.

■ ASSOCIATED CONTENT

Ⓢ Supporting Information

Theoretical estimation of line width broadening due to graphene and experimental data on the effect of ion-gel on the cavity resonance. This material is available free of charge via the Internet at http://pubs.acs.org.

■ AUTHOR INFORMATION

Corresponding Author
*E-mail: fengwang76@berkeley.edu.

Author Contributions
‖These authors contributed equally.

Notes
The authors declare no competing financial interest.

■ ACKNOWLEDGMENTS

■ REFERENCES

(1) Miller, D. *Proc. IEEE* **2009**, *97* (7), 1166−1185.

(2) Wang, F.; Zhang, Y.; Tian, C.; Girit, C.; Zettl, A.; Crommie, M.; Shen, Y. R. *Science* **2008**, *320* (5873), 206−209.

(3) Li, Z. Q.; Henriksen, E. A.; Jiang, Z.; Hao, Z.; Martin, M. C.; Kim, P.; Stormer, H. L.; Basov, D. N. *Nat. Phys.* **2008**, *4* (7), 532−535.

(4) Liu, M.; Yin, X.; Ulin-Avila, E.; Geng, B.; Zentgraf, T.; Ju, L.; Wang, F.; Zhang, X. *Nature* **2011**, *474* (7349), 64−67.

(5) Gu, T.; Petrone, N.; McMillan, J. F.; van der Zande, A.; Yu, M.; Lo, G. Q.; Kwong, D. L.; Hone, J.; Wong, C. W. *Nat. Photonics* **2012**, *6* (8), 554−559.

(6) Gan, X.; Mak, K. F.; Gao, Y.; You, Y.; Hatami, F.; Hone, J.; Heinz, T. F.; Englund, D. *Nano Lett.* **2012**, *12*, 5626−5631.

(7) Furchi, M.; Urich, A.; Pospischil, A.; Lilley, G.; Unterrainer, K.; Detz, H.; Klang, P.; Andrews, A. M.; Schrenk, W.; Strasser, G.; Mueller, T. *Nano Lett.* **2012**, *12* (6), 2773−2777.

(8) Engel, M.; Steiner, M.; Lombardo, A.; Ferrari, A. C.; Löhneysen, H. v.; Avouris, P.; Krupke, R. *Nat. Commun.* **2012**, *3*, 906.

(9) Gan, X.; Shiue, R.-J.; Gao, Y.; Mak, K. F.; Yao, X.; Li, L.; Szep, A.; Walker, D., Jr.; Hone, J.; Heinz, T. F.; Englund, D. *arXiv:1211.0458*, **2012**.

(10) Noda, S.; Fujita, M.; Asano, T. *Nat. Photonics* **2007**, *1* (8), 449−458.

(11) Li, X.; Cai, W.; An, J.; Kim, S.; Nah, J.; Yang, D.; Piner, R.; Velamakanni, A.; Jung, I.; Tutuc, E.; Banerjee, S. K.; Colombo, L.; Ruoff, R. S. *Science* **2009**, *324* (5932), 1312−1314.

(12) Kim, K. S.; Zhao, Y.; Jang, H.; Lee, S. Y.; Kim, J. M.; Kim, K. S.; Ahn, J.-H.; Kim, P.; Choi, J.-Y.; Hong, B. H. *Nature* **2009**, *457* (7230), 706−710.

(13) Kim, B. J.; Jang, H.; Lee, S.-K.; Hong, B. H.; Ahn, J.-H.; Cho, J. H. *Nano Lett.* **2010**, *10* (9), 3464−3466.

(14) Englund, D.; Majumdar, A.; Faraon, A.; Toishi, M.; Stoltz, N.; Petroff, P.; Vučković, J. *Phys. Rev. Lett.* **2010**, *104* (7), 073904.

(15) Buffeteau, T.; Grondin, J.; Danten, Y.; Lassègues, J.-C. *J. Phys. Chem. B* **2010**, *114* (22), 7587−7592.

(16) Kim, J.; Son, H.; Cho, D. J.; Geng, B.; Regan, W.; Shi, S.; Kim, K.; Zettl, A.; Shen, Y.-R.; Wang, F. *Nano Lett.* **2012**, *12* (11), 5598−5602.

(17) Emani, N. K.; Chung, T.-F.; Ni, X.; Kildishev, A. V.; Chen, Y. P.; Boltasseva, A. *Nano Lett.* **2012**, *12* (10), 5202−5206.

(18) Falkovsky, L. A. *Physics-Uspekhi* **2008**, *51* (9), 887.

(19) Novoselov, K. S.; Geim, A. K.; Morozov, S. V.; Jiang, D.; Katsnelson, M. I.; Grigorieva, I. V.; Dubonos, S. V.; Firsov, A. A. *Nature* **2005**, *438* (7065), 197−200.

(20) Zhang, Y.; Tan, Y.-W.; Stormer, H. L.; Kim, P. *Nature* **2005**, *438* (7065), 201−204.

(21) Cho, J. H.; Lee, J.; Xia, Y.; Kim, B.; He, Y.; Renn, M. J.; Lodge, T. P.; Daniel Frisbie, C. *Nat. Mater.* **2008**, *7* (11), 900−906.

(22) Chen, C.-F.; Park, C.-H.; Boudouris, B. W.; Horng, J.; Geng, B.; Girit, C.; Zettl, A.; Crommie, M. F.; Segalman, R. A.; Louie, S. G.; Wang, F. *Nature* **2011**, *471* (7340), 617−620.

(23) Faraon, A.; Majumdar, A.; Kim, H.; Petroff, P.; Vučković, J. *Phys. Rev. Lett.* **2010**, *104* (4), 047402.

(24) Sukang, B.; Hyeong Keun, K.; Xianfang, X.; Jayakumar, B.; Tian, L.; Young Il, S.; Young Jin, K.; Barbaros, O.; Jong-Hyun, A.; Byung Hee, H.; Sumio, I. *CORD Conference Proceedings*, **2009**.